Electronics and Electrical Engineering

Research article

An experimental analysis of fuzzy logic-sliding mode based IFOC controlled induction motor drive

Rekha Tidke* and Anandita Chowdhury

Sardar Vallabhbhai National Institute of Technology, Surat India

* **Correspondence**: Email: rstidke@gmail.com.

Abstract: This paper presents the prototyping of a fuzzy logic-sliding mode control technique for improved dynamics of induction motors. The proposed technique used the new fuzzy logic-sliding mode control technique as the main drive control using indirect field-oriented control theory. A simulation model was designed and implemented in a MATLAB/Simulink environment. An experimental prototype of the proposed circuit topology was fabricated, with a 0.37 kW induction motor fed from a quasi-impedance source inverter (q-ZSI) controlled by fuzzy logic-sliding mode-based indirect field-oriented control. In the real-time control, a DSpace 1202 Microlab box was used as a deployment module for the new control scheme on the q-ZSI-fed induction motor. The performance was studied under various constant speed ranges and step/ramp speed responses, both in simulations and experimentally. In this study, the proposed control method showed improved dynamic behavior of the system under constant speed and forward speed operation. The impact of FL-SMC in speed tracking with fast speed convergence was validated with experimental results. Moreover, ripple-free voltage and the current of the induction motor were observed with the proposed control scheme.

Keywords: induction motor; fuzzy logic; sliding mode control; electric vehicle; DSpace

1. Introduction

Recently, there has been a rapid increase in electric vehicle (EV) utility, which may also increase exponentially in the near future. Most urban developing areas of all countries are opting for EVs to replace conventional internal combustion (IC) engine vehicles. The EV drive is achieved by different types of electrical motors, particularly alternating current (AC) motors, which display good

performance. AC motors can be divided into two categories: permanent magnet synchronous motors (PMSM) or induction motor (IM). The former is a common option for non-commercial vehicles. The induction motor is extensively used in industrial applications due to its reliability, effectiveness, and easy installation and maintenance. The availability of high-power electronic converters with mature technology and the advantages of IMs makes it the most suitable choice for EV or hybrid EV (HEV) applications. When compared with IM, the PMSM is an economical and efficient solution for EV/EHV, and e-vehicle manufacturers mostly use PMSM and IM motors in the propulsion drive system.

The construction of PMSM and brushless DC motors requires a permanent magnet on the rotor, which is expensive and needs to be imported. Also, there are viable substitutes that rely on rare earth magnets for vehicle propulsion systems: induction and synchronous motors. A comparison, selection, and review of different propulsion motors for EV/HEV are explained in [1,2], and there are several available studies done on induction motor speed control and other machines, like PMSMs (permanent magnet synchronous motor) and SRMs (switched reluctance motor). In [3], a speed control was applied to the induction motor and connected to a quasi-z-source indirect matrix converter. The voltage transfer ratio was improved, enhancing the performance of the induction motor. The machine voltage was boosted to higher values during voltage sag conditions, maintaining the speed of the machine. To control the quasi-z-source matrix converter, a space vector pulse width modulation (PWM) was used. In [4], a vector control was proposed for controlling the speed of the induction motor connected to a quasi-z-source direct matrix converter (QZSDMC). The QZSDMC was controlled by a variable duty ratio shoot-through control method to adjust the voltage output of the inverter. The QZSDMC could be operated in buck and boost modes by changing the duty ratio of the shoot-through control. The induction motor was controlled with an indirect field–oriented control algorithm, which performed better even during full-load conditions. The speed of the motor varied dynamically at different instants of time, validating the performance of the machine by using a simulation and an experimental setup.

In [5], the PMSM speed was controlled by a novel fuzzy fractional-order PID controller. The membership functions were modeled as per the speed range requirement of the EV PMSM. An optimization control technique was introduced for the estimation of parameters of the fuzzy logic controller as per real time consideration. The proposed control module attained optimum speed control of the PMSM, with reference signals generated by the fuzzy fractional-order PID controller.

In EV systems, the power converter plays a vital role in increasing the input and stage of DC-AC conversion. Furthermore, it is required to achieve different speed ranges with speed monitoring and battery-managing systems. The conventional voltage source inverter (VSI) requires a high DC input voltage to accomplish the desired output voltage, causing the system to gain weight and loose power if operated with less input voltage, hence reducing overall efficiency, which is undesirable for EV systems. The quasi-ZSI (q-ZSI) can work with less input, as it has a built-in boost converter due to its impedance network. The unique feature of q-ZSI—DC-DC and DC-AC conversion in a single stage—makes it the most suitable converter for EV application, eliminating the drawbacks of conventional VSI [6–8].

The q-ZSI combines the advantages of the basic ZSI and its unique abilities: It provides continuous current and a reduced burden on the input source. Moreover, the reduced quantity of components with lower ratings makes it cost-effective. The various applications of q-ZSI-fed IM drives found in EV/HEV applications, fuel cells, photovoltaic panel, or PV arrays, among others, are discussed in [9,10]. To an improved dynamic performance, propulsion systems require efficient power converters along with an upgraded control drive. The q-ZSI shows flexibility in hybrid energy

storage through a battery and supercapacitor for the IM-drive system. A hybrid control strategy composed of two main basic control methods for EV systems was discussed in [11,12]. In [13,14], a PMSM drive was controlled by a q-ZSI with a single current sensor control module. The speed range of the PMSM was extended as the voltage range of the QZSI increased, which is very helpful for electric vehicle applications.

In [15–17], the sliding mode control (SMC) was used in combination with direct torque control (DTC) and indirect field-oriented control (IFOC) techniques. The SMC provides improved dynamic transient response and displays an ability to sustain transients for parameter variation and external disturbances. The torque ripple causes the vibration in the system that leads to the premature wear of the drive components; the induction motor may then suffer from torsional oscillations due to torque ripples. The fuzzy logic is easy to implement and, in combination with a PI controller, can overcome the higher deviation and longer response time of the system. In [18], a novel control approach was presented for IM speed control with q-ZSI. An electric power drive system is most suitable for an EV/HEV system when appropriately chosen, as addressed by [19]; however, torque and flux ripples, along with steady-state errors, can occur due to the use of a PI speed controller. In [20], AI techniques (FLC, ANN along with PI, and PI-SMC) were used in IM drive for EV/HEV applications. The SMC controller will generate oscillations around the sliding-mode surfaces (chattering), damaging the actuators. For this reason, a FLC-SMC speed controller was implemented in [21]. The fuzzy logic, along with field-oriented control, were implemented to improve speed control, as FLC shows better performance than a PID controller. Fuzzy logic control is easy to implement with any control technique for performance improvement [22]. Important features required for speed control are load variations and sensitivity to motor parameters. These advantages are guaranteed with the SMC and the fuzzy logic algorithm to minimize the chattering phenomenon. The authors in [23] showed the effectiveness of the SMC-FL combination in achieving fast response and good parameter control through simulation results. A sensorless speed control scheme was implemented for the IM drive, using SMC for sensorless speed control. With decoupled flux and rotor speed, it uses two SMC controllers. Also, the author in [24] mentioned the stability, robustness, and tracking control for the system. In both acceleration and deceleration modes of operation, the ZSI-fed IM is efficiently used for electric vehicles (EVs) [25]. The author in [26] elaborated on the different rules of fuzzy controller performance for speed control of induction motors, investigating a superior performance with 49 rules of fuzzy logic.

The conventional techniques, which include only PI controllers, have a higher settling time and slower response rates. Because of this, optimal control of the machine is not achieved, and the speed of the machine has higher damping. In the hybrid control technique, the matured IFOC scheme is used for decoupled control, with the IM fed from q-ZSI and FL-SMC. The proposed technique gives an improved dynamic response with convergence of speed.

This paper is arranged as follows: The proposed test module is introduced in Section 1, followed by the design of the proposed fuzzy logic-sliding mode module in Section 2. Section 3 includes the simulation results with different operating conditions. This simulation is validated by a prototype experimental setup with lower rating, and the results are shown in Section 4. The final Section 5 concludes the paper, determining the best control module for the operation of IM in different operating conditions.

2. Proposed controller design

The indirect field-oriented control (IFOC) technique primarily requires a controlled motor speed

and regulated 3-phase stator currents to generate pulses to the inverter. To achieve advanced optimal speed control, the conventional PI current controllers in the traditional IFOC are replaced by a fuzzy logic-sliding mode. One of the main advantages of SMC is its ability to maintain stability and ensure tracking of the desired trajectory even in the presence of uncertainties and disturbances. The sliding surface is designed in such a way that it is insensitive to certain types of uncertainties. The fuzzy logic control adjusts the current at each step based on the current error and its rate of change. However, the fuzzy logic control approach may suffer from ripples in the stator flux and torque, both during dynamic transient and steady-state conditions. Hence, the combination of FL-SMC overcomes these disadvantages.

In the FLC technique, the triangular membership function (MF) for the input variables is necessary to decrease the computational load and speed up the process. Every input has seven membership functions, so 49 fuzzy control rule possibilities. In Table 1, the negative big, negative medium, and negative small are named NB, NM, and NS, respectively; zero is ZE; positive big, positive medium, and positive small are PB, PM, and PS, respectively. The fuzzy logic produced two controlled and optimized current values, i_{ds_FL} and i_{qs_FL}, that help in ripple reduction and eliminating chattering of SMC.

Table 1. Fuzzy membership functions.

$e\, i_{qs_{ref}}$ / $e^* i_{qs\_ref}$	NB	NM	NS	ZE	PS	PM	PB
NB	NB	NB	NB	NB	NM	NS	ZE
NM	NB	NB	NB	NM	NS	ZE	PS
NS	NB	NB	NM	NS	ZE	PS	PM
ZE	NB	NM	NS	ZE	PS	PM	PB
PS	NM	NS	ZE	PS	PM	PB	PB
PM	NS	ZE	PS	PM	PB	PB	PB
PB	ZE	PS	PM	PB	PB	PB	PB

The d-axis and q-axis current regulators need to be tuned. The control of these two currents is done by FL-SMC. Two sliding surfaces are required, s_1 and s_2; one is for i_{ds} control, and the other one is for i_{qs} control.

$$s_1 = i_{ds\_ref} - i_{ds} \tag{1}$$

$$s_2 = i_{qs\_ref} - i_{qs} \tag{2}$$

Where i_{ds_ref} and i_{qs_ref} are the reference values.

The control law is designed for the current regulator.

$$v_{ds} = V_{ds}^{equ} + V_{ds}^{n} \tag{3}$$

$$v_{qs} = V_{qs}^{equ} + V_{qs}^{n} \tag{4}$$

The voltage discontinuous control V_{ds}^{n} and V_{qs}^{n} is defined as

$$V_{ds}^n = k_1 \; sat \left(\frac{s_1}{\varphi_1}\right) \tag{5}$$

$$V_{qs}^n = k_2 \; sat \left(\frac{s_2}{\varphi_2}\right) \tag{6}$$

$$sat \left(\frac{s_1}{\varphi_1}\right) = \begin{cases} \dfrac{s_1}{\varphi_1} \; ; & if \; \left|\dfrac{s_1}{\varphi_1}\right| < 1 \\ sign \left(\dfrac{s_1}{\varphi_1}\right) \; ; & if \; \left|\dfrac{s_1}{\varphi_1}\right| > 1 \end{cases} \tag{7}$$

$$sat \left(\frac{s_2}{\varphi_2}\right) = \begin{cases} \dfrac{s_2}{\varphi_2} \; ; & if \; \left|\dfrac{s_2}{\varphi_2}\right| < 1 \\ sign \left(\dfrac{s_2}{\varphi_2}\right) \; ; & if \; \left|\dfrac{s_2}{\varphi_2}\right| > 1 \end{cases} \tag{8}$$

Where k_1, k_2 are positive constant, and the constant factor φ_1, φ_2 are the "boundary layer values". The simplified current equations are used to get an equivalent voltage control law V_{ds}^{equ} and V_{qs}^{equ} [17]

$$\frac{di_{ds}}{dt} = \frac{1}{L_s \, \sigma}[V_{ds} - R_\sigma \, i_{ds} + \frac{L_m}{L_r} \frac{1}{t_r} \psi_{dr} + \frac{L_m}{L_r} \; \omega_m \, \psi_{qr} + L_s \, \sigma \, \omega_e i_{qs}] \tag{9}$$

$$\frac{di_{qs}}{dt} = \frac{1}{L_s \, \sigma} [V_{qs} - R_\sigma \, i_{qs} + \frac{L_m}{L_r} \frac{1}{t_r} \psi_{qr} - \frac{L_m}{L_r} \; \omega_m \, \psi_{dr} - L_s \, \sigma \, \omega_e i_{ds}] \tag{10}$$

Where $R_\sigma = [R_s + \frac{L_m^2}{t_r \, L_r}]$ and $\sigma = \left[1 - \frac{L_m^2}{L_s \, L_r}\right]$ and $t_r = \frac{L_r}{R_r}$.

Where V_{ds}, V_{qs}, i_{ds}, i_{qs}, ψ_{ds} and ψ_{qs} are stator d-axis and q-axis voltage, current, and flux, respectively. ψ_{dr}, ψ_{qr} are rotor d-axis and q-axis flux. R_s, R_r, L_m, L_r and P are the IM motor parameters stator resistance, rotor resistance, mutual inductance, rotor inductance, and pole pairs, respectively.

The derivative of sliding surface s_1 and s_2 is given below

$$\dot{s_1} = \dot{i_{ds\_ref}} - \dot{i_{ds}} \tag{11}$$

$$\dot{s_2} = \dot{i_{qs\_ref}} - \dot{i_{qs}} \tag{12}$$

$\dot{s_1} = 0$ and $\dot{s_2} = 0$ for equivalent control law
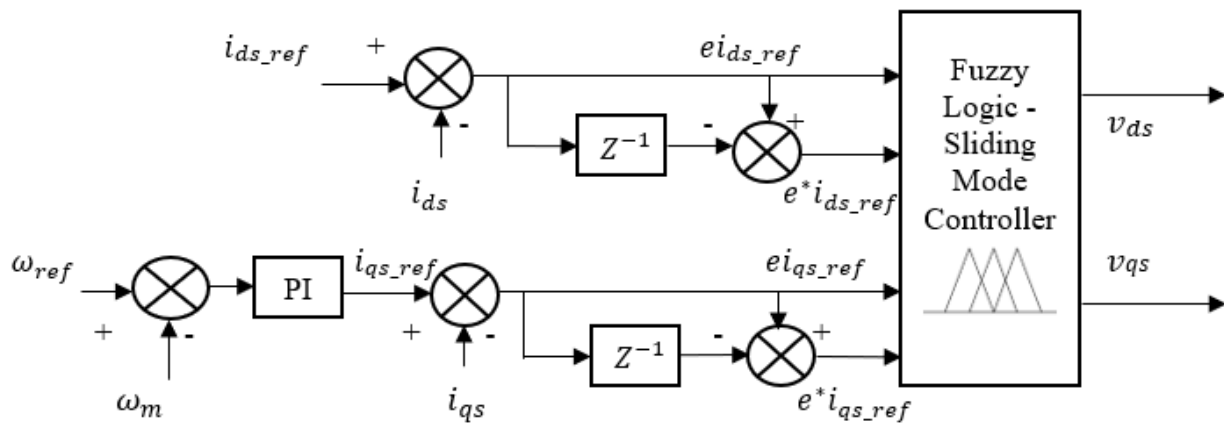
Figure 1. Proposed FL-SMC controller schematic.

In Figure 1, Z^{-1} is a MATLAB delay function. The proportional-integral (PI) compares the actual and reference speed for controlling speed error signal. The final voltage equivalent control law values are obtained with the help of fuzzy logic-controlled current values.

$$V_{ds}^{equ} = L_s \, \sigma \, [i_{ds_{FL}}^{\cdot} + \frac{1}{L_s \, \sigma} R_\sigma i_{ds} - \frac{1}{L_s \, \sigma} \frac{L_m}{L_r} \frac{1}{t_r} \psi_{dr\_ref} - \omega_e i_{qs}] \tag{13}$$

$$V_{qs}^{equ} = L_s \, \sigma \, [i_{qs\_FL}^{\cdot} + \frac{1}{L_s \, \sigma} R_\sigma i_{qs} + \frac{1}{L_s \, \sigma} \frac{L_m}{L_r} \omega_m \, \psi_{dr\_ref} + \omega_e i_{ds}] \tag{14}$$
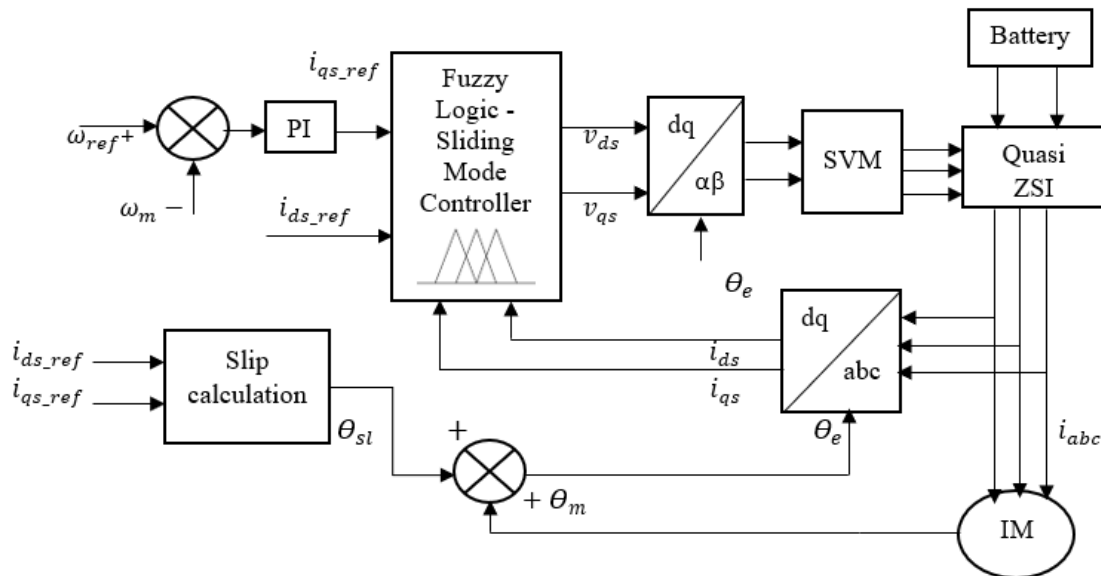
Figure 2. Proposed control scheme block diagram.

In the proposed hybrid control technique, the speed PI controller is combined with FL-SMC for speed control (Figure 2). The fuzzy logic (FL) is merged with SMC for direct and quadrature axis current control. FL-SMC is applied to investigate the behavior of the IM drive with the proposed control technique. The FL-SMC shows fast speed tracking and reduces ripple. Moreover, it ensures that the system converges and stays on the desired trajectory, even if there are uncertainties affecting

the system.

The IM drive is supplied by a q-ZSI. The q-ZSI addresses the issue of discontinuous input current of traditional Z-source inverters (ZSI), which can adversely affect battery life and the performance of EVs and HEVs. By rearranging the components of the Z-source network, the q-ZSI is created, providing continuous input current. The q-ZSI performs two-stage DC-DC-AC conversion in a single stage, offers wide voltage buck-boost capabilities, and is more advantageous than conventional VSI. Its ability to extend the output voltage range and reduce component requirements makes it an efficient and cost-effective solution for EVs and HEVs.

3. Software simulations and results

According to the system modeling and design of the proposed fuzzy logic-sliding mode-based IFOC for the IM, the modeling is conducted using the MATLAB Simulink tool. A squirrel cage IM is used for testing the proposed control method in MALTAB Simulink.

Table 2. Specification of IM for simulation.

| Mutual inductance	0.172 H
Stator inductance	0.178 H
Rotor inductance	0.178 H
Stator resistance	1.405 ′Ω
Rotor resistance	1.395 ′Ω
Pole pairs	2
Rated power	4 kW
Rotor rated speed	1430 rpm
Rated voltage	400 V

3.1. Performance analysis of the proposed system at constant speed operation

For the performance analysis of the proposed controller on IM drive with the specifications mentioned in Table 2, it was operated at a constant reference rotor speed in rad/sec and constant load toque in Nm. The analysis of the proposed system was observed through simulation waveform using the MATLAB Simulink environment.
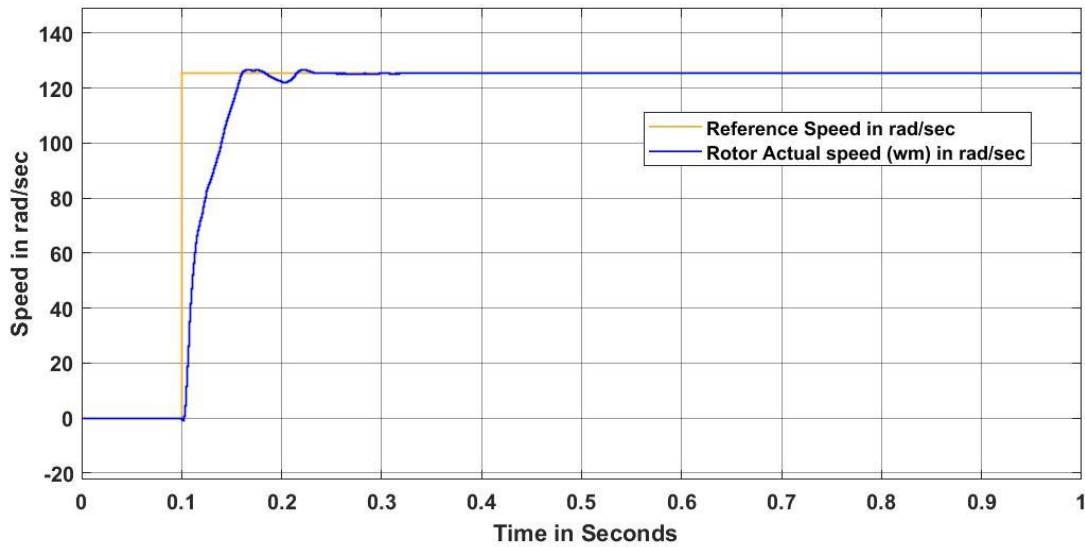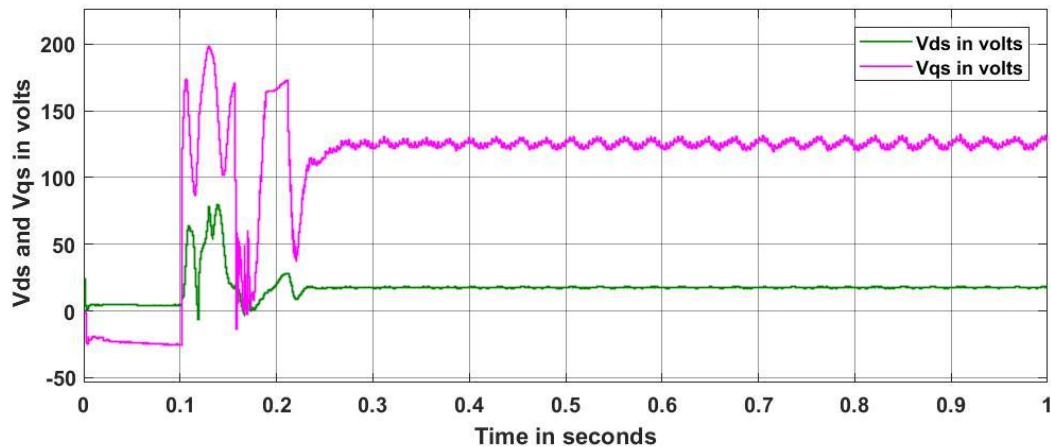
Figure 3. Speed response under constant speed operation.

Under the constant speed operation, the proposed control system for the IM drive was simulated from a standstill condition to a constant speed of 125 rad/sec (1200 rpm) with a 10 Nm load torque. The MATLAB simulated results of the constant speed response are shown in Figure 3. It can be observed from the speed response of the proposed control system that the actual rotor speed smoothly reaches the set reference speed. The standstill condition lasts from 0 to 0.1 s, after which the speed transitions to 125 rad/sec. It has been observed that after standstill condition, the speed converges in less than 0.3 s (settling from 0.1 to 0.4 s). The speed curve shows good dynamic response under the constant speed operation of the proposed control method.
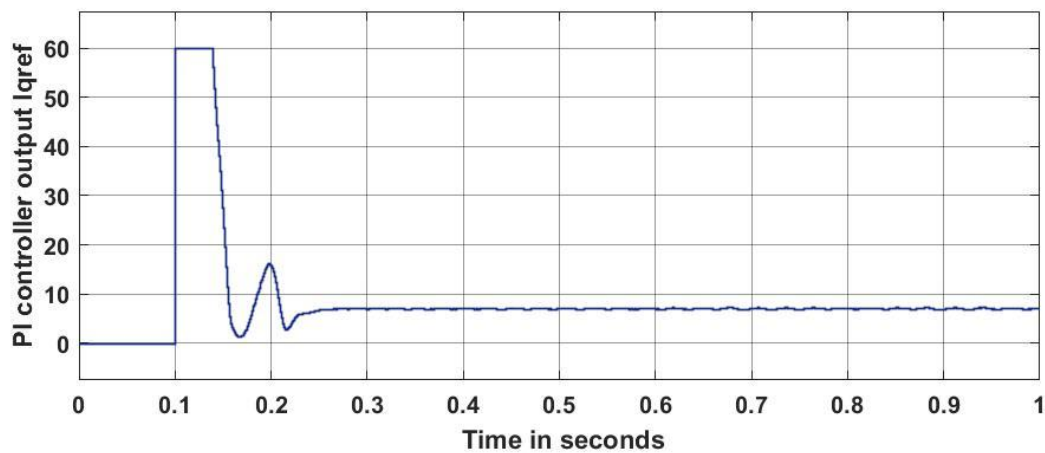
Figure 4. Speed PI controller output as Iqref under the constant speed operation.

Figure 5. Vds and Vqs response under the constant speed operation.

Moreover, it was also observed that the speed PI controller output gives a constant value, as required by the controller, as shown in Figure 4. At standstill conditions, it outputs zero value, and at switchover point, its oscillates and settles down to Iqref. The fuzzy logic-sliding mode controller is used to provide direct and quadrature axis voltages, as shown in Figure 5. It was observed from the voltage response of the FL-SMC controller that the chattering issue is reduced, and well-controlled output voltages are achieved.

3.2. Performance analysis of the proposed system under the forward and reverse speed operation

Under the forward and reverse speed operation, the proposed control system of IM drive was simulated from standstill conditions to different operating speeds. The MATLAB simulated result of wide speed range response is shown in Figure 6.
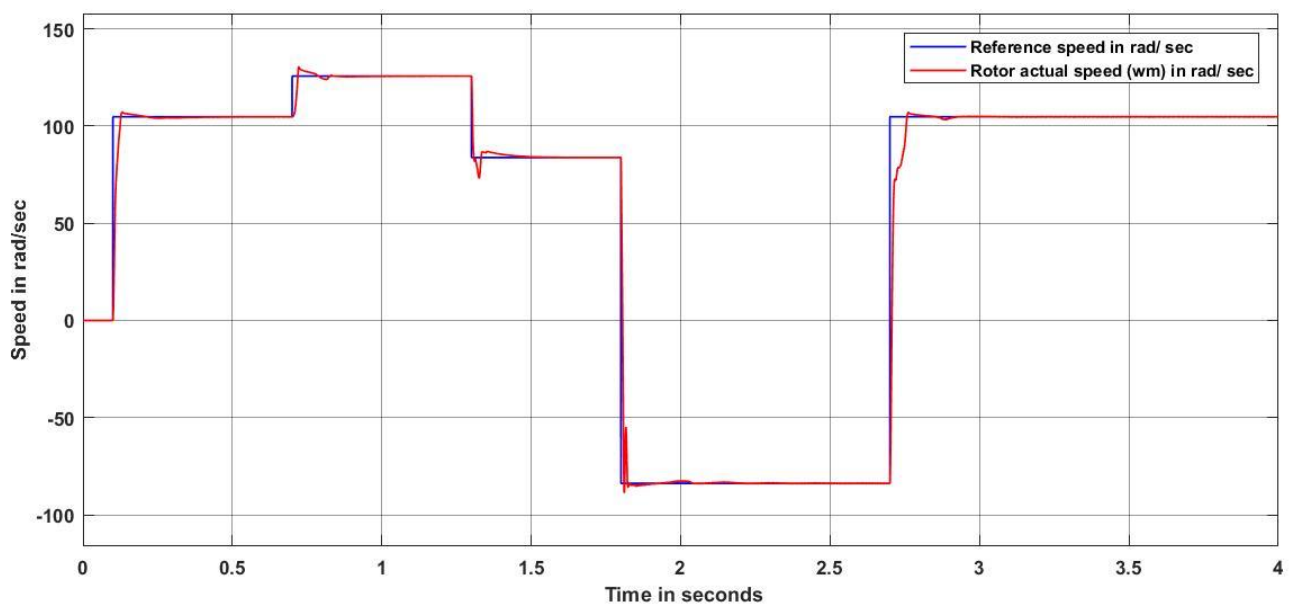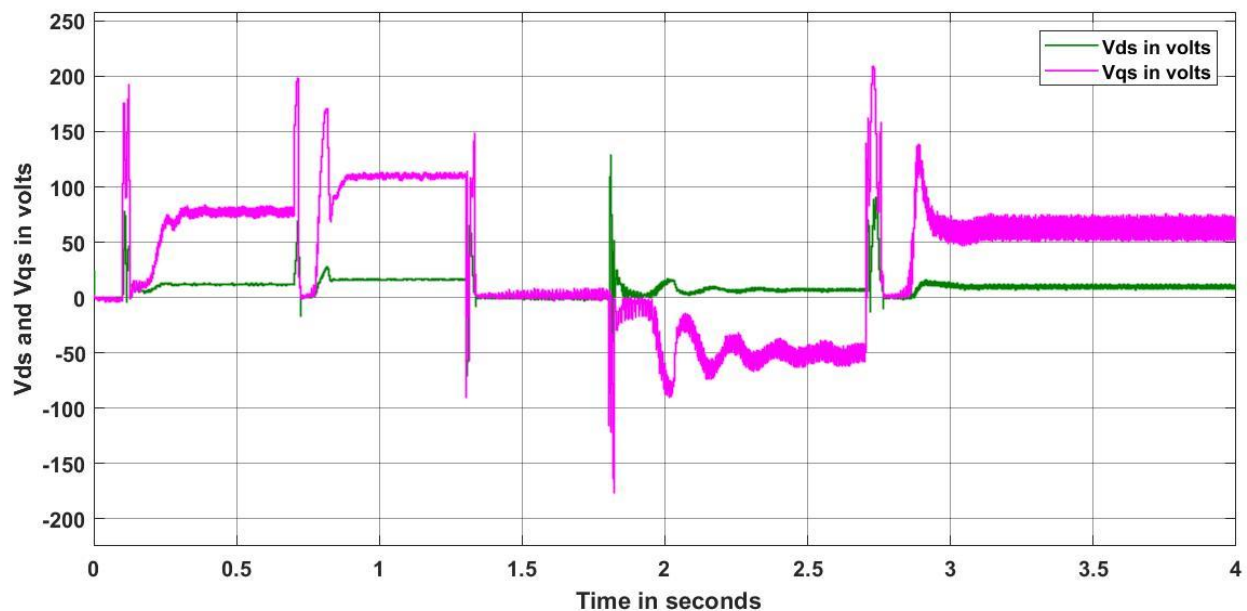

Figure 6. Speed response under the forward and reverse speed operation.

The reference speed was initially set at standstill, followed by a step-up to forward speeds ranging from 0 rad/sec to 104.7 rad/sec to 125.6 rad/sec in acceleration mode for the EV. Subsequently, the speed decreased from 125.6 rad/sec to 83.7 rad/sec in deceleration mode for the EV. The speed reversal condition was also set from 83.7 rad/sec to -83.7 rad/sec. It was observed from the speed response that the actual rotor speed converges to the set reference speed under all speed conditions: forward speed operation, speed decreased operation, and speed reversal operation. Moreover, it took 0.3 to 0.35 s for convergence. A smooth dynamic response has been observed during forward and reverse speed operation.
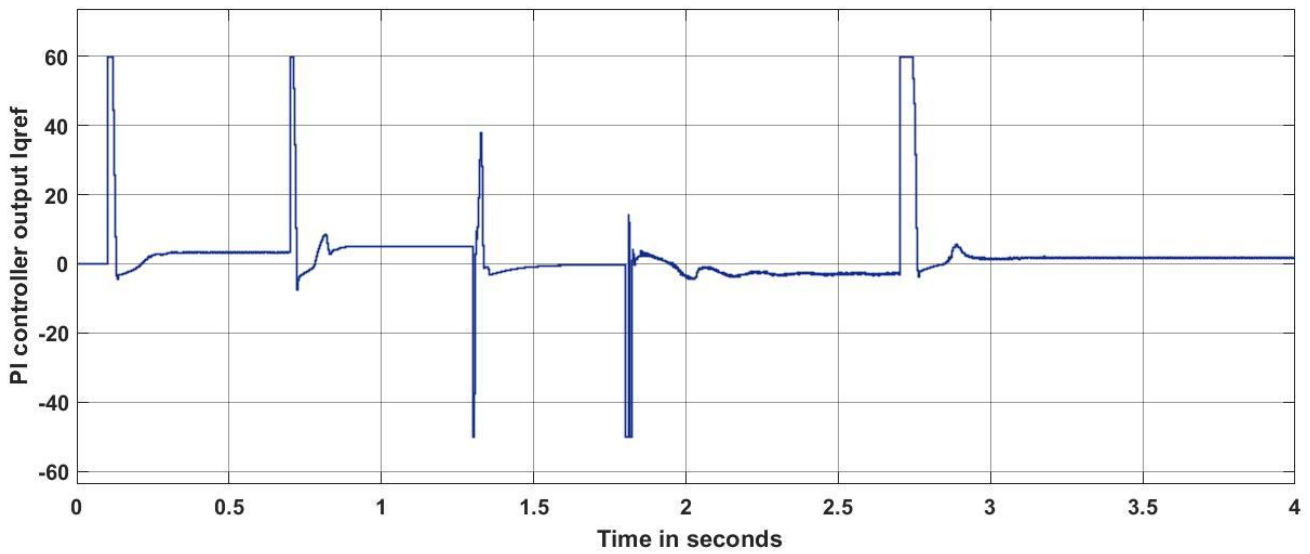
Figure 7. Speed PI controller output as Iqref under the forward and reverse speed operation.

Figure 8. Vds and Vqs response under the forward and reverse speed operation.

Furthermore, a Iqsref waveform in Figure 7 and the direct-quadrature axis voltage waveform shown in Figure 8 were observed. From the waveforms, the Iqsref was controlled to achieve different

speed conditions. Similarly, the voltages of the IM drive were controlled by the FL-SMC controller. During forward speed operation, both iqs_ref and Vqs reversed polarities, while only the magnitude changed in other parameters. During the transition from one speed condition to another, increased and decreased magnitude were seen before convergence.

4. System prototyping and results

4.1. System description

To validate the simulation results from the previous section, an experimental setup was fabricated with a prototype design (Figure 9). The controller was deployed to the external module DSpace 1202 Microlab box. For prototyping, a small squirrel cage IM was used, with the following specifications: P_{rated} = 0.37 kW, V_{rated} = 220 V, Rs = 10.794 Ω, Ls = 0.7238 H, Rr = 9.613 Ω, Lr = 0.77109 H, Lm = 0.6864 H, N_{rated} = 1430 rpm, pole pairs = 2.

The inverter receives firing signals from SVPWM pulses generated by the DSpace RTI 1202. The 3-phase squirrel cage IM was equipped with a simple loading arrangement and speed encoder placed at the shaft. Analog incremental encoder output pulses are input into the DSpace via digital I/O pins to capture speed. A 3-phase hall current sensor is used to capture the 3-phase current of the induction motor. The output of the current sensor is input to DSpace via analog channels. The host PC is equipped with MATAB software 2014b and DSpace control desk to monitor real-time output results.
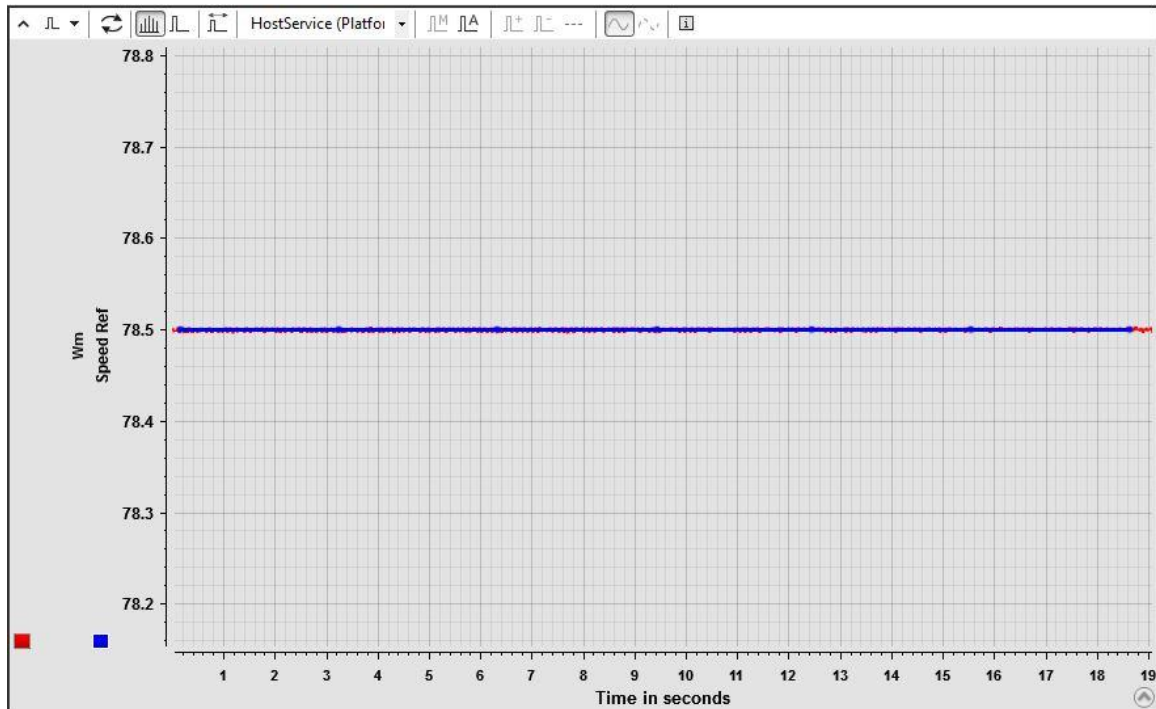

Figure 9. Prototype model of proposed system.

The experiment was conducted for different speed references with slight loading conditions.

A. Performance of the proposed system at constant speed

A prototype model of the proposed system with IM was tested at a constant reference speed of 750 rpm (78.5 rad/sec).

**Figure 10.** Result of speed response under constant speed operation.

A prototype result of the proposed control IM model was obtained using DSpace RTI 1202 control desk, as shown in Figure 10. It was observed that the proposed control method provides smooth speed control. The results show that speed converges at set speed.
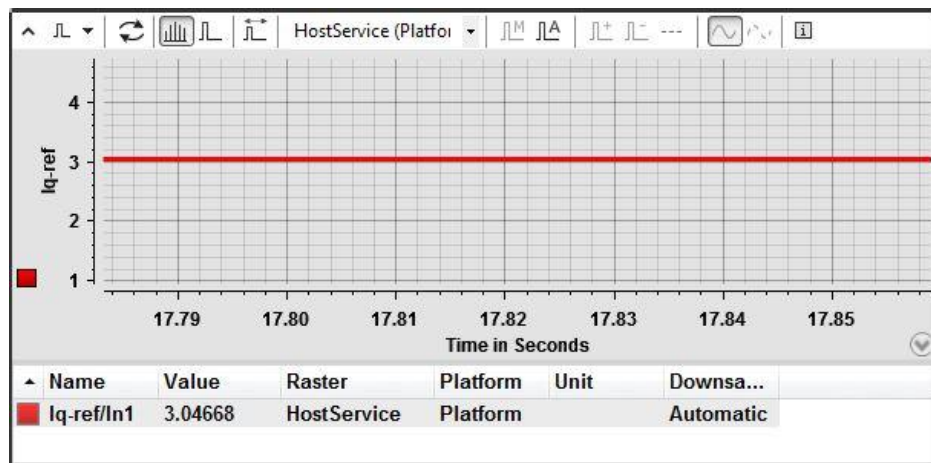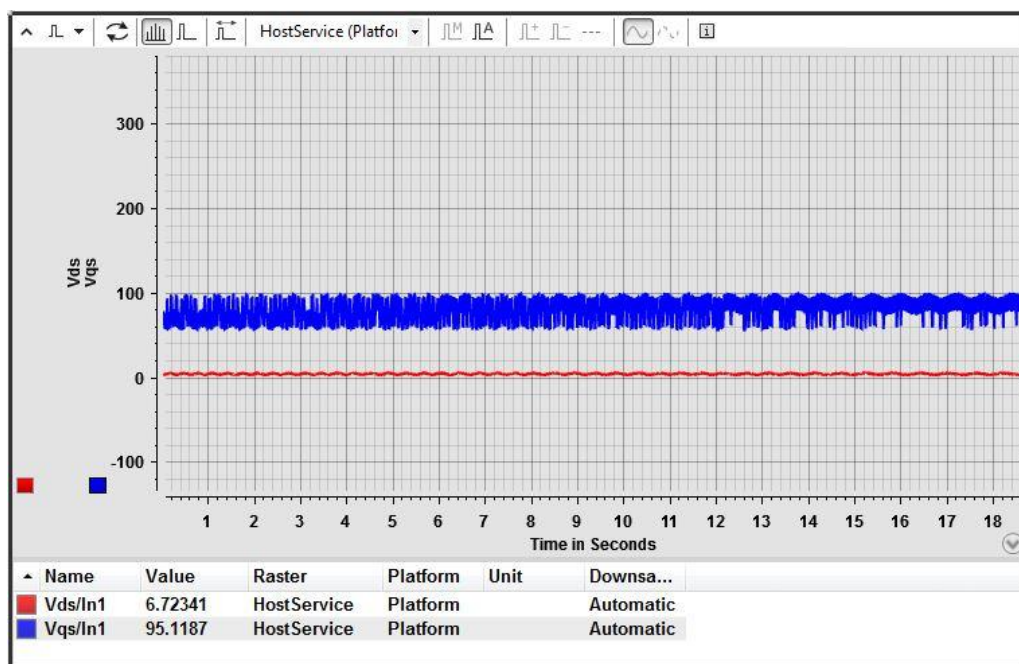

Figure 11. Result Iqsref under constant speed operation.

The PI controller outputs a constant result as Iqsref, as shown in Figure 11, which is used as input to the FL_SMC controller. The fuzzy logic works using if-else rules, employing two inputs and seven membership functions, with 49 fuzzy rules implemented. A fuzzy logic control approach suffers from ripple content in stator flux and torque under dynamic conditions. The FL-SMC reduces this ripple and achieves fast speed tracking. Moreover, controlled firing pulses can be seen in Figure 12. From the pulse zoom view, the generated frequency is observed to be 25 Hz.
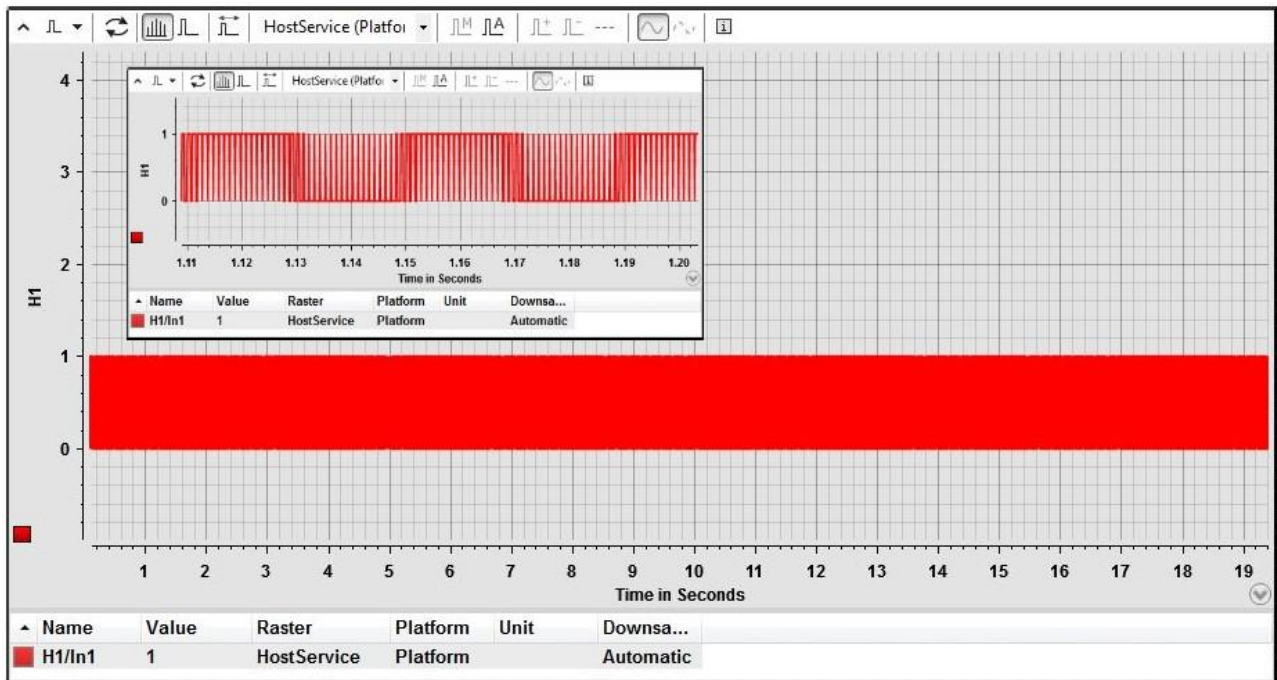
Figure 12. Result of gate firing pulses under constant speed operation.

**Figure 13.** Result of FL-SMC controlled Vqs and Vds under constant speed operation.

The FL-SMC-controlled voltages are observed in Figure 13. Vqs shows reduced distortion in the waveform; however, Vds shows an insignificant distorted waveform. These consistently controlled voltages provide the required alpha-beta voltages, as shown in Figure 14. Upon closer observation of the zoom view in Figure 14, voltages exhibit reduced ripple in the waveform. The prototype model was tested across various constant speed ranges and consistently showed speed convergence.
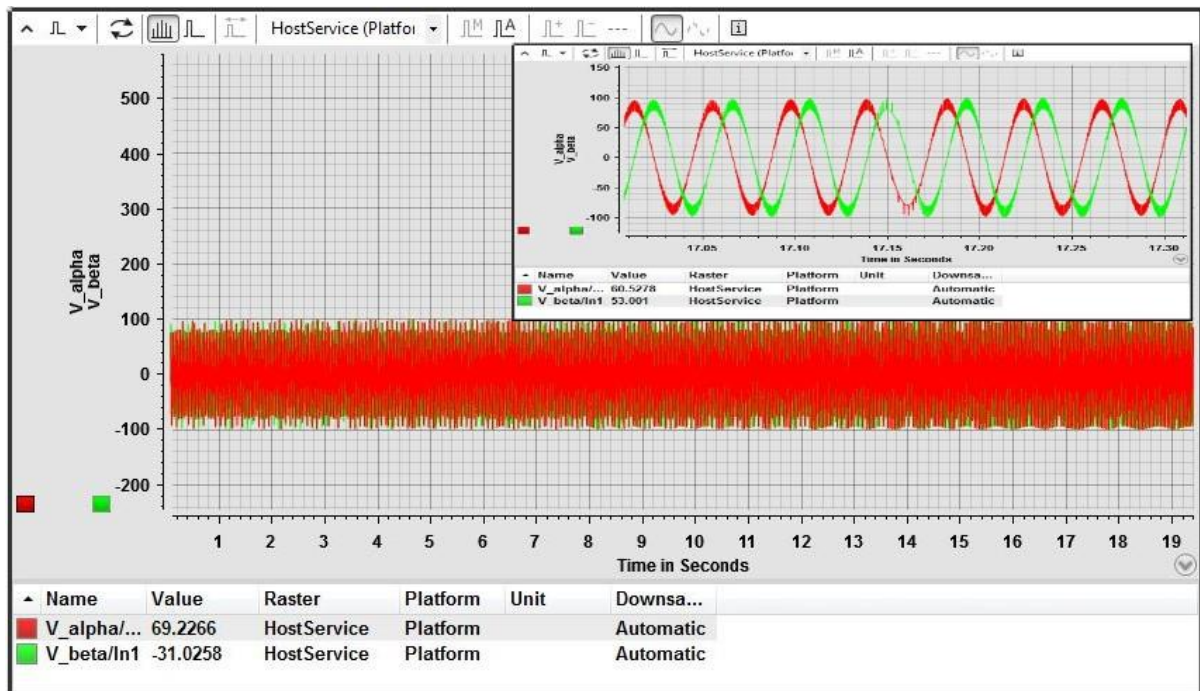
Figure 14. Result of V_alpha and V_beta voltage under constant speed operation.

B. Performance of the proposed system under speed forward condition

The prototype model was tested for speed change response using a slider in control desk for real-time speed change.
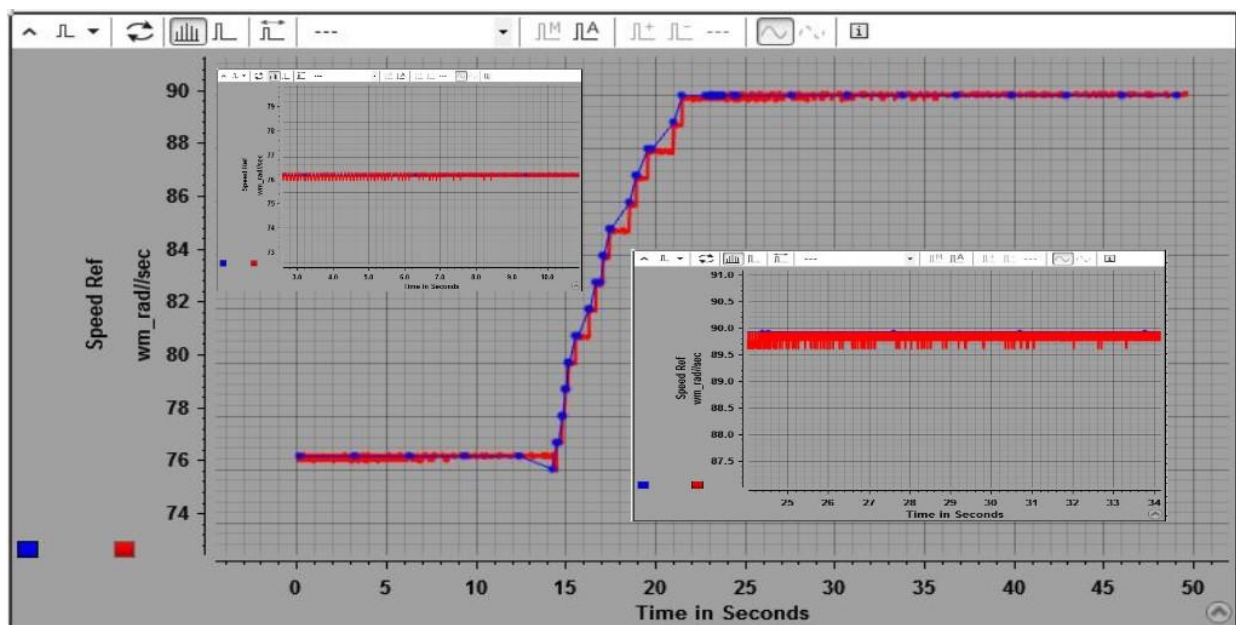

Figure 15. Result for speed changes in forward (ramp) operation under forward speed operation.

For speed change, the set speed gradually increases from one speed to another using a slider while the motor is running. It has been observed from the real-time speed change response that the proposed system converges to the set speed, as shown in Figure 15. In the zoom view, both initial

and final speeds are shown.

Figure 16 shows the real-time gate pulse waveform, where the pulse period (hence frequency) changes automatically controlled by the FL-SMC control algorithm. It has been observed that the control pulses from SVPWM are used to fire the q-ZSI switches, which provides the required voltage and current to the induction motor. Zoom view 1 shows the initial stage of pulses, and zoom view 2 shows the final pulses after the set speed change.


Zoom view 1   Zoom view 2
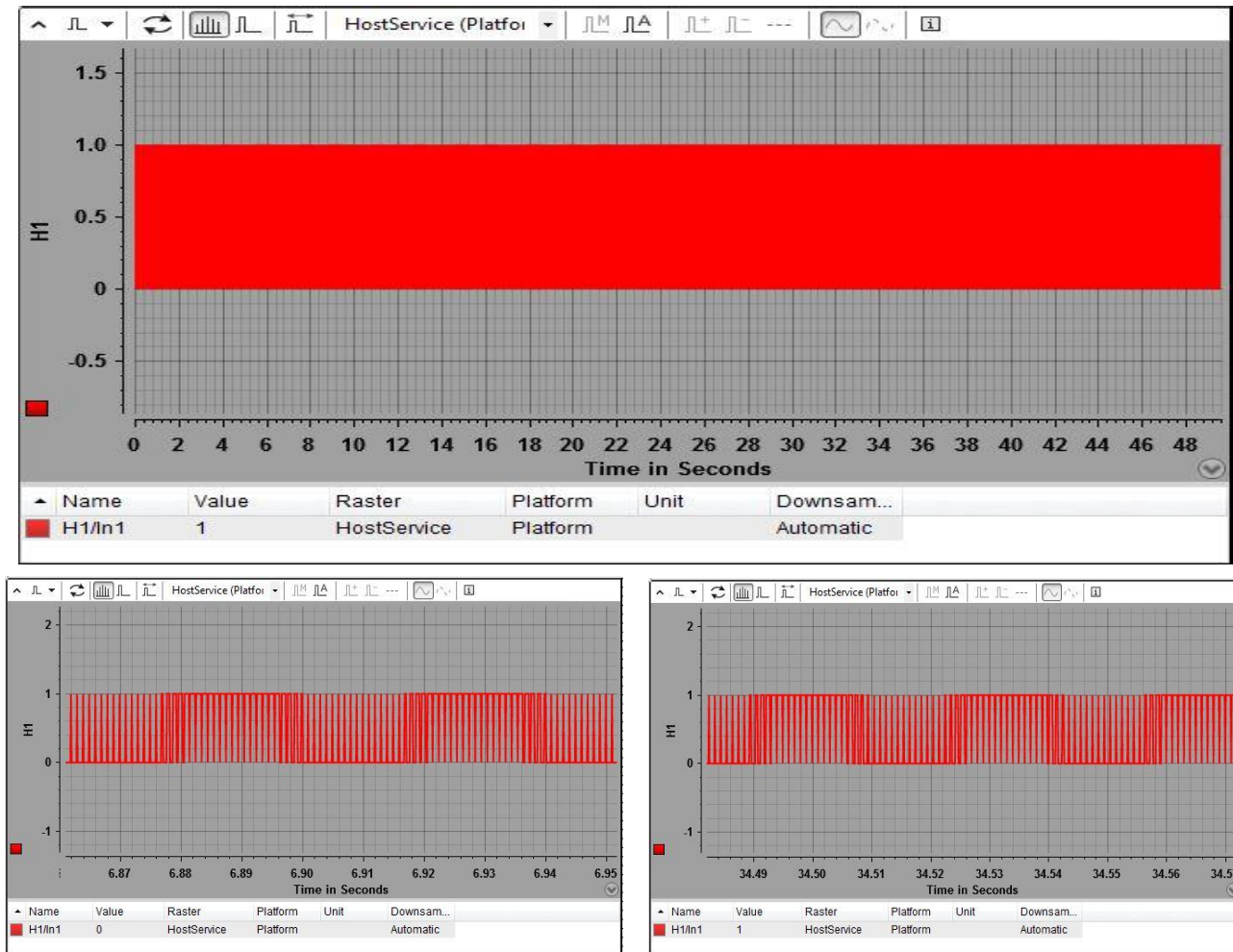
Figure 16. Result for firing gate pulses at ramp speed response under forward speed operation.
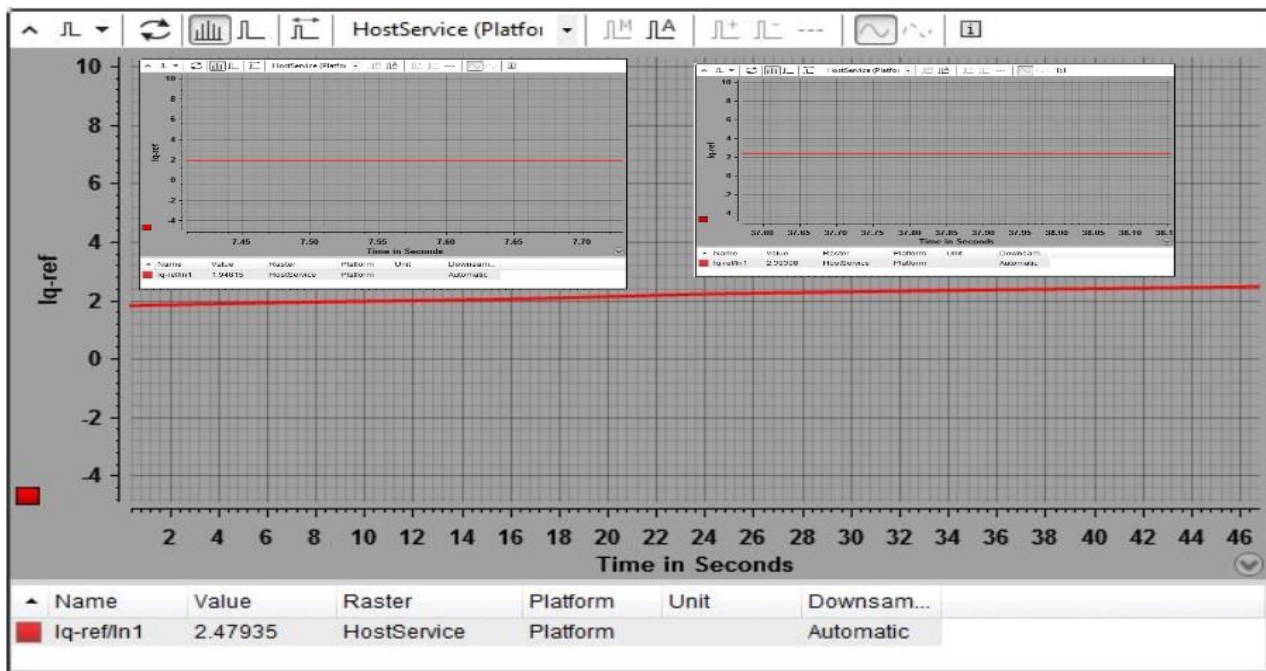
Figure 17. Result of Iqsref response under forward speed operation.

As the speed gradually increases, the same is reflected in the PI controller Iqsref, which increases slightly as shown in Figure 17. Furthermore, changes in the pulse period and frequency can be observed for the inverter. From the zoom view in both parts, it is observed that a reduced ripple is seen in the waveform.
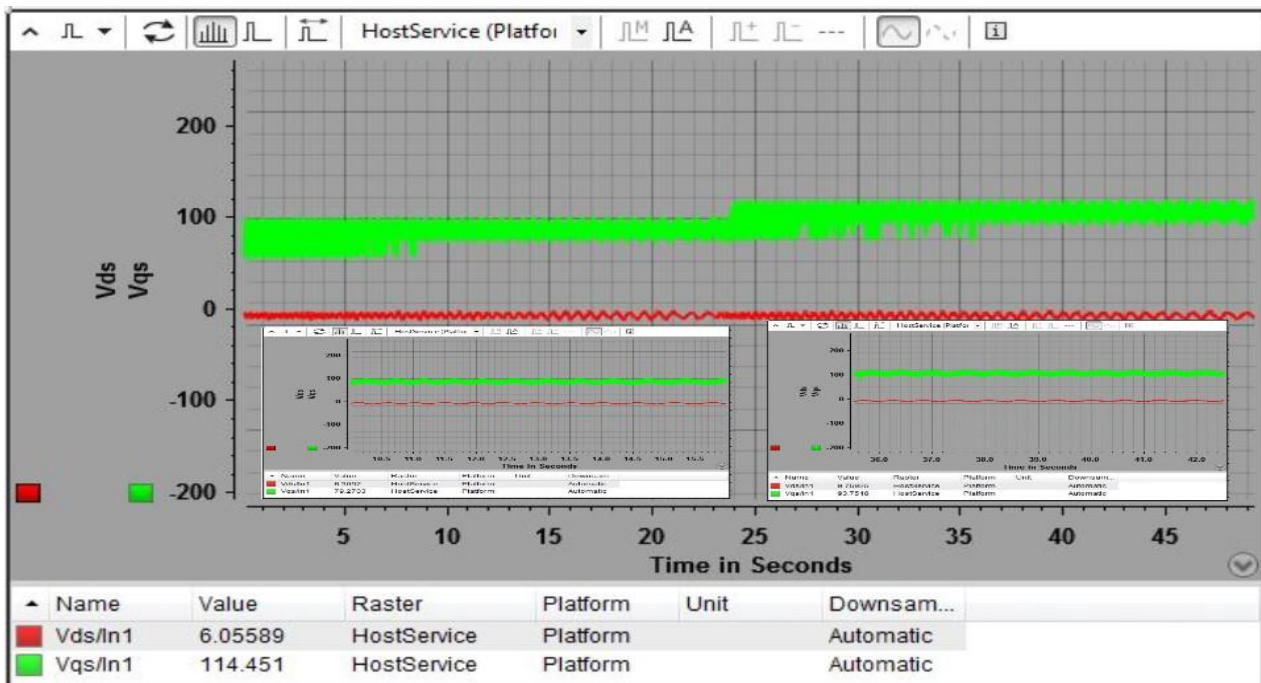
Figure 18. Result of FL-SMC-controlled Vqs and Vds under forward speed operation.
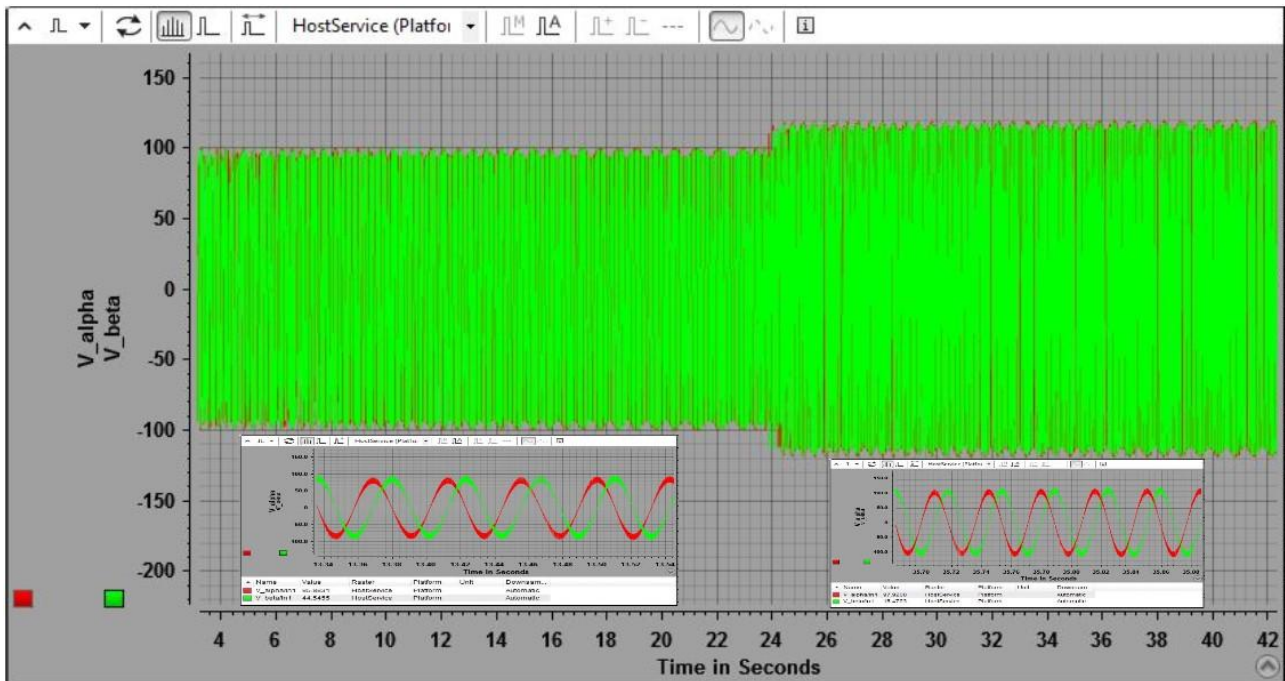
Figure 19. Result of V_alpha and V_beta voltage under forward speed operation.

Moreover, the FL-SMC-controlled voltages are seen in Figure 18. At the initial stage, the Vqs value ranges from 75 to 90 V and then from 95 to 115 V. It has been observed that speed control of the quadrature axis voltage is crucial. These controlled voltages and the slip speed from Iqsref are utilized to obtain controlled alpha- beta voltages, as shown in Figure 19. Clear waveforms are seen in the zoom view for both initial and change points. Moreover, smooth, and ripple-free voltages are observed in Figure 19.

In the experimental analysis of the proposed control method for IM drive, a dynamic response was observed. The prototype model operated under constant reference speed, constant load torque, and speed change conditions. The DSpace RTI 1202 provided real-time results for the analysis of FL-SMC-controlled IM drive. Under constant speed and forward speed operation, the proposed control system improves dynamic responses in terms of speed tracking, fast speed convergence, and reduction in ripple in both speed and voltage current of the induction motor.

5. Conclusions

In this paper, a new control technique was implemented for IM drive appropriate for EV/HEV drive applications. The proposed FL-SMC control technique gives an improved dynamic response, as seen on the MTALAB Simulink environment under constant speed and under forward reverse speed operations. An acceleration, deceleration, and speed reversal mode has been investigated for speed convergence and speed tracking in extensive speed ranges and load variations. The experimental results using a prototype model validate the simulation results. Moreover, FL-SMC significantly reduces ripple in speed, current, and voltage, as observed in simulation waveforms; however, in hardware results, fast speed tracking and convergence were evident under constant speed and under forward speed operations. The FL-SMC achieved smooth speed waveform and reduced ripple. Also, the reduction in ripple in voltage and current responses revealed an improved dynamic performance

of the induction motor.

6. Future scope

The hardware investigation may be carried out under acceleration, deceleration, and speed reversal modes. Under load variation, it is necessary to observe the compatibility of the proposed control scheme in real time. A comparative study can be suggested in hardware with conventional IFOC method.

Author contributions

Rekha Tidke: Conceptualization, Software, Investigation, Methodology, Validation, Writing – original draft, Writing – review & editing; Anandita Chowdhury: Conceptualization, Supervision, Writing – original draft, Writing – review & editing. All authors have read and agreed to the published version of the manuscript.

Use of AI tools declaration

The authors declared they have not used Artificial Intelligence (AI) tools in the creation of this article.

Conflict of interest

The authors declare that there is no conflict of interest in this paper.

References

1. Gor CP, Shah VA, Gor MP (2016) Electric vehicle drive selection related issues. *2016 International Conference on Signal Processing, Communication, Power and Embedded System (SCOPES)*, 74–79. https://doi.org/10.1109/SCOPES.2016.7955554
2. Popescu M, Goss J, Staton DA, Hawkins D, Chong YC, Boglietti A (2018) Electrical Vehicles—Practical Solutions for Power Traction Motor Systems. *IEEE T Ind Appl* 54: 2751–2762. https://doi.org/10.1109/TIA.2018.2792459
3. Vidhya DS, Venkatesan T (2017) Quasi-Z-Source Indirect Matrix Converter Fed Induction Motor Drive for Flow Control of Dye in Paper Mill. *IEEE T Power Electr* 33: 1476–1486. https://doi.org/10.1109/TPEL.2017.2675903
4. Ellabban O, Abu-Rub H, Ge B (2014) A Quasi-Z-Source Direct Matrix Converter Feeding a Vector Controlled Induction Motor Drive. *IEEE J Em Sel Top Power Electr* 3: 339–348. https://doi.org/10.1109/JESTPE.2014.2309979
5. George MA, Kamat DV, Kurian CP (2021) Electronically Tunable ACO Based Fuzzy FOPID Controller for Effective Speed Control of Electric Vehicle. *IEEE Access* 9: 73392–73412. https://doi.org/10.1109/ACCESS.2021.3080086
6. Tong WP, Ramadan BM, Logenthiran T (2018) A Comparative Analysis between Z-Source and Quasi-Z-Source Inverters for Boost Operation. *2018 Asian Conference on Energy, Power and Transportation Electrification (ACEPT)*, 1–6. https://doi.org/10.1109/ACEPT.2018.8610771

7. Maity T, Prasad H (2017) Real-time performance evaluation of quasi z-source inverter for induction motor drives. *2017 IEEE 26th International Symposium on Industrial Electronics (ISIE)*, 844–849. https://doi.org/10.1109/ISIE.2017.8001356

8. Siwakoti YP, Peng FZ, Blaabjerg F, Loh PC, Town GE (2014) Impedance-Source Networks for Electric Power Conversion Part I: A Topological Review. *IEEE T Power Electr* 30: 699–716. https://doi.org/10.1109/TPEL.2014.2313746

9. Rahman S, Rahman K, Ali MA, Meraj M, Iqbal A (2019) Quasi Z Source Inverter Fed V/f Controlled Five Phase Induction Motor Drive Powered. *2019 International Conference on Electrical, Electronics and Computer Engineering (UPCON)*, 1–6. IEEE. https://doi.org/10.1109/UPCON47278.2019.8980073

10. Telrandhe ST, Pande SS, Umredkar SV (2019) Performance Analysis of Solar Fed Electronically Commutated Motor Driven Water Pump Using ZSI and q-ZSI. *2019 3rd International Conference on Computing Methodologies and Communication (ICCMC)*, 157–161. https://doi.org/10.1109/ICCMC.2019.8819660

11. Muhammad M, Rasin Z, Jidin A (2019) Bidirectional Quasi-Z-Source Inverter with Hybrid Energy Storage for IM Drive System. *2019 IEEE 9th Symposium on Computer Applications & Industrial Electronics (ISCAIE)*, 75–80. https://doi.org/10.1109/ISCAIE.2019.8743869

12. Farasat M, Trzynadlowski AM, Fadali MS (2014) Efficiency improved sensorless control scheme for electric vehicle induction motors. *IET Electr Syst Transp* 4: 122–131. https://doi.org/10.1049/iet-est.2014.0018

13. Xiao S, Shi T, Li X, Wang Z, Xia C (2018) Single-current-sensor control for PMSM driven by quasi-Z-source inverter. *IEEE T Power Electr* 34: 7013–7024. https://doi.org/10.1109/TPEL.2018.2875533

14. Xiao S, Gu X, Wang Z, Shi T, Xia C (2019) A Novel Variable DC-Link Voltage Control Method for PMSM Driven by a Quasi-Z-Source Inverter. *IEEE T Power Electr* 35: 3878–3890. https://doi.org/10.1109/TPEL.2019.2936267

15. Saghafinia A, Ping HW, Uddin MN, Gaeid KS (2014) Adaptive Fuzzy Sliding-Mode Control Into Chattering-Free IM Drive. *IEEE T Ind Appl* 51: 692–701. https://doi.org/10.1109/TIA.2014.2328711

16. Ghezouani A, Gasbaoui B, Ghouili J (2018) Modeling and Sliding Mode DTC of an EV with Four In-Wheel Induction Motors Drive. *2018 International Conference on Electrical Sciences and Technologies in Maghreb (CISTEM)*, 1–9. https://doi.org/10.1109/CISTEM.2018.8613379

17. Nasri A, Gasbaoui B, Fayssal BM (2016) Sliding mode control for four wheels electric vehicle drive. *Procedia Technology* 22: 518–526. https://doi.org/10.1016/j.protcy.2016.01.111

18. Fereka D, Zerikat M, Belaidi A (2018) MRAS Sensorless Speed Control of an Induction Motor Drive based on Fuzzy Sliding Mode Control. *2018 7th International Conference on Systems and Control (ICSC)*, 230–236. https://doi.org/10.1109/ICoSC.2018.8587844

19. Zechmair D, Steidl K (2012) Why the induction motor could be the better choice for your electric vehicle program. *World Electric vehicle Journal* 5: 546–549. https://doi.org/10.3390/wevj5020546

20. Sami I, Ullah S, Basit A, Ullah N, Ro JS (2020) Integral Super Twisting Sliding Mode Based Sensorless Predictive Torque Control of Induction Motor. *IEEE Access* 8: 186740–186755. https://doi.org/10.1109/ACCESS.2020.3028845

21. Nguyen-Vinh Q, Pham-Tran-Bich T (2023) Slidingmode control of induction motor with fuzzy logic observer. *Electr Eng* 105: 2769–2780. https://doi.org/10.1007/s00202-023-01842-2

22. Ariff RM, Hanafi D, Utomo WM, Ching KB, Zin NM, Sim SY, et al. (2013) Fuzzy Logic Control Design for Induction Motor Speed Control Improvement through Field Oriented Control. *Information Technology Convergence: Security, Robotics, Automations and Communication* 253: 273–280. https://doi.org/10.1007/978-94-007-6996-0_29

23. Ettalabi1 N, Bouzi M, Bossoufi B, Anoune K, Mouncef E (2020) Fuzzy-Sliding Mode Speed Control of Permanent Magnet Synchronous Motor Using NPC Converter. *International Journal of Engineering Research and Technology* 13: 1649–1657. https://doi.org/10.37624/IJERT/13.7.2020.1649-1657

24. Quan NV, Long MT (2022) Sensorless sliding mode control method for a three-phase induction motor. *Electr Eng* 104: 3685–3695. https://doi.org/10.1007/s00202-022-01578-5

25. Jyothi B, Bhavana P, Sarada K, Srikanth M (2020) Analysis of Z-Source Inverter fed Asynchronous Motor for Electric Vehicle Applications. *IOP Conf. Series: Materials Science and Engineering* 993: 012087. https://doi.org/10.1088/1757-899X/993/1/012087

26. Farah N, Talib MH, Ibrahim Z, Abdullah Q, Aydoğdu Ö, Azri M, et al. (2021) Investigation of the Computational Burden Effects of Self-Tuning Fuzzy Logic Speed Controller of Induction Motor Drives With Different Rules Sizes. *IEEE Access* 9: 155443–155456. https://doi.org/10.1109/ACCESS.2021.3128351